Clinical, pharmacology and in vivo studies of QingDai (indigo naturalis) promotes mucosal healing and symptom improvement in ulcerative colitis by regulating the AHR-Th17/Treg pathway

Sizhen Gu[1†], Yan Xue[2†], Xiaowen Liu[1], Yini Tang[3], Dong Wang[4], Dongmei Wu[5], Mingrong Yao[6], Zehua Xia[7], Sen Yang[8], Gan Cai[9], Shigui Xue[3*] and Danbo Dou[1*]

Abstract

Qingdai (QD), derived from various plant sources, is commonly used in traditional Chinese medicine for ulcerative colitis (UC) treatment. However, the clinical efficacy and mechanisms of orally administered QD remain unclear. This study aims to evaluate QD's efficacy in UC treatment and uncover its active components and mechanisms. A randomized controlled trial compared QD to Adisa, followed by UPLC-Q-TOF/MS and network pharmacology analyses to identify QD's core components and targets. In vivo experiments on a UC mouse model explored QD's impact on the AHR-Th17/Treg pathway using PCR, WB, ELISA, and flow cytometry. Results showed QD's efficacy in UC treatment, with mucosal healing and remission comparable to Adisa. UPLC-Q-TOF/MS identified 16 core components in mouse colon tissue, with network pharmacology revealing 67 targets, potentially involving the IL-17 signaling pathway and Th17 cell differentiation. QD and its components up-regulated AHR, CYP1A1, and Foxp3, while down-regulating RORγt. Additionally, QD modulated pro-inflammatory (IL-6, IL-17 A) and anti-inflammatory (IL-10, TGF-β1) factors, and Treg/Th17 cell ratios in LPMC. Oral QD administration effectively promoted mucosal healing and improved UC symptoms, potentially through AHR-Th17/Treg pathway regulation.

Keywords Ulcerative Colitis, Qingdai, Clinical efficacy, UPLC-Q-TOF-MS, AHR, Th17/Treg

[†]Sizhen Gu and Yan Xue contributed equally to this work.

*Correspondence:
Shigui Xue
sidney2009@163.com
Danbo Dou
doudanbo@shutcm.edu.cn

Full list of author information is available at the end of the article

Introduction

Ulcerative colitis (UC) is a chronic inflammatory bowel disease characterized by recurrent inflammation of the colon and rectum mucosa. This debilitating condition presents with a spectrum of symptoms, including abdominal pain, diarrhea, rectal bleeding, and weight loss, significantly impairing the quality of life for affected individuals. The etiology of UC remains multifactorial, involving a complex interplay between genetic predisposition, environmental factors, and dysregulation of the immune system. Furthermore, patients with UC who fail to control inflammatory activities for an extended period face a higher risk of intestinal cancer, with the overall cancer rate reaching 0.81% [1]. Currently, first-line drugs for treating UC include 5-aminosalicylic acid, hormones, immunosuppressants, and biological agents (such as anti-TNF-α, integrin α4β7 antagonists, and JAK inhibitors) [2–4]. Despite the availability of numerous treatment options, there are still some patients who do not respond or experience side effects such as opportunistic infections, bone marrow suppression, and carcinogenesis. Therefore, many UC patients are still seeking simpler, more efficient, affordable, and safer treatment options.

Traditional Chinese medicine (TCM) has emerged as a promising avenue for exploring novel therapeutic options for UC [5]. QingDai (QD) is a unique traditional Chinese medicine (TCM), which is a dried plant powder extracted from the leaves of several plants, including the perennial herb Strobilanthes cusia (Ness) W. Ktze. of the Acanthaceae, the annual herb Polygonum tinctorium Ait. of the Polygonaceae, and the biennial herb Isatis indigotica Fortune of the Brassicaceae and has been traditionally used to treat dysentery and bloody stools [6]. In previous clinical studies of UC, QD was used as an enema or suppository [7]. However, more recent studies have shown that both compound formulations containing QD [8–11] and single-drug QD preparations [12–14], when taken orally, can promote mucosal healing under colonoscopy. Oral administration is more convenient and avoids the discomfort associated with other delivery methods. Nevertheless, clinical studies on oral QD have some design limitations, such as single-arm studies, short observation periods, and high confounding factors, which result in a lower level of evidence-based support. Additionally, adverse events associated with oral QD have been observed, indicating that its safety profile still requires further optimization.

In addition, the metabolic process of QD in vivo and the specific mechanism of treating UC are not clear at present. Studies have found that the increasing incidence of inflammatory bowel disease in recent years may be related to a decrease in the intake of green vegetables rich in indole [15]. Given that QD is rich in indole, some believe it can be used as a dietary supplement for green vegetables. Our research group has previously explored the efficacy of QD in treating ulcerative colitis (UC) using an integrated approach that includes GEO gene chip analysis, network pharmacology, and molecular docking techniques. We found that the therapeutic impact of QD on UC may be attributed to its role in activating the body's systemic immune response [16]. Moreover, the indole in QD can serve as a ligand for Aryl Hydrocarbon Receptor (AHR) in vivo [17]. AHR is a transcription factor that can be activated by exogenous ligands and participate in multiple important biological processes in the body [18–20]. Numerous in vitro and in vivo studies have confirmed that the activation of AHR helps to balance the ratio between regulatory T cells (Treg) and helper T cells 17 (Th17), thus maintaining the stability of the intestinal mucosa [21]. The imbalance between Treg and Th17 is closely related to the pathogenesis of UC. In UC patients, the number of Th17 cells increases significantly, while the number and function of Treg cells decrease, leading to immune system imbalance and intestinal inflammation. By activating AHR, the number and function of Treg cells can be increased, thereby inhibiting the excessive activation of Th17, relieving intestinal inflammation, and promoting the treatment of UC. However, it is still unclear whether QD corrects Th17/Treg imbalance and repairs intestinal mucosa to treat UC through AHR.

Therefore, in this study, we confirmed that a lower dosage of QD remains clinically as effective as Adisha in treating UC. Additionally, we identified the key active components of QD and verified that these core components can alleviate UC through the AHR-Th17/Treg signaling pathway.

Methods and materials

Clinical study

Clinical trial design and participants

This investigation employed a multicenter, open-label, randomized controlled design with a focus on non-inferiority, and was conducted at Shuguang Hospital affiliated with Shanghai University of TCM, Shanghai First People's Hospital, and Baoshan Integrated Traditional Chinese and Western Medicine Hospital. The study protocol was received an approval from the Ethics Committee of Shuguang Hospital affiliated to Shanghai University of Traditional Chinese Medicine (Approval No. 2023-1405-172-01) and registered with the Chinese Clinical Trial Registry (Registration No. ChiCTR2000035497). The study protocol adhered to the principles outlined in the Declaration of Helsinki. All participants were recruited from inpatient and outpatient clinics at Shuguang Hospital affiliated with Shanghai University of TCM from October 2020 to December 2021. And written informed consent was obtained from all participants prior to their inclusion in the study.

Enrolled patients, aged 18 to 65 years, were diagnosed with ulcerative colitis (UC) based on the diagnostic criteria established by the Inflammatory Bowel Disease (IBD) group of the Chinese Society of Gastroenterology (GSC). Inclusion required a modified Mayo score (MMS) falling within the range of 3 to 10 (on a scale of 0–12, where higher scores denote increased disease severity). Exclusion criteria comprised individuals with infectious colitis, Crohn's disease, ischemic enteritis, radiation enteritis, severe UC complications, or other significant systemic illnesses. The study also excluded disabled individuals, pregnant or breastfeeding women, and participants concurrently involved in other clinical drug trials.

Clinical trial data collection and assessment
The patients' demographic data and disease characteristics were collected before randomization. Colonoscopy were conducted both within the week preceding intervention and at 16-week mark. Endoscopic disease activity was assessed by trained colonoscopies utilizing modified Mayo endoscopic score (MMES). Clinical disease activity was assessed by trained physicians, employing the MMS and the short inflammatory bowel disease questionnaire (SIBDQ). Venous blood samples were obtained from each patient at weeks 0 and 16, with blood tests encompassing erythrocyte sedimentation rate (ESR) and C-reactive protein (CRP) levels. The primary efficacy endpoint focused on the mucosal healing rate following 16 weeks of treatment. The MMES, initially determined by assessing the most severe site at baseline, was reevaluated in the same area after the 16-week intervention. Mucosal healing was defined as a MMES of ≤1.

The main secondary efficacy endpoint was the rate of clinical remission and endoscopic response after 16 weeks of treatment. Endoscopic response was defined as a decrease in the MMES by at least 1 point from baseline. Clinical remission was specified as a MMS≤2 with no subscores exceeding 1. Furthermore, changes in the MMS, partial Mayo score, MMES, SIBDQ score, ESR levels, and CRP levels were determined by comparing the values obtained after 16 weeks of treatment with the baseline values.

Clinical trial drug preparation
Powdered QD from consistent batches (Fujian Province, China; Chinese Good Manufacturing Practice Drug Certification No. FJ20180005) were purchased from Shanghai TCM Pharmaceutical Technology Co. LTD (Shanghai, China). Quantification of QD compounds was detailed in Figure S1 and Table S1. Prior to encapsulation, the powdered QD (Figure S2A) underwent sterilization, and a multi-residue pesticide analysis confirmed the absence of residual agricultural chemicals. The encapsulation process involved adding the sterilized powdered QD to white-coated capsules (100 mg per capsule; Figure S2B) at Shanghai Traditional Chinese Medicine Pharmaceutical Technology Co. LTD (Shanghai, China). Ai-Di-Sha (ADS; 500 mg per bag; Product batch number: 160603) consisted of mesalazine sustained-release granules and was made by Shanghai Ethypharm Co., Ltd. (China).

Clinical trials sample size determination and randomization
The sample size was determined based on the calculation of a non-inferiority trial design. Mucosal healing rates from previous reports were 46% for QD and 29.7% for ADS. In our study, using $\alpha=0.05$, $\beta=0.1$, and a boundary value of 0.07, eligible patients were assigned to QD and ADS groups in a 1:1 ratio, employing the Z-test for comparison. Considering a 10% dropout rate, the calculated minimum sample size was 30 participants per group. Randomization into the two groups was performed by a statistician from the Good Clinical Practice (GCP) Center of Shuguang Hospital affiliated with Shanghai University of Traditional Chinese Medicine, utilizing computer-generated random tables. The QD group received one capsule of QD twice a day, while the ADS group took eight bags of ADS daily for 16 weeks. The participant flowchart was presented in Figure S3.

Pharmacology Study
Preparation of serum of mice after QD intervention
We purchased 20 SPF C57BL/6 male mice from Shanghai Bi kai Experimental Animal Co., Ltd. All mice were accommodated in a controlled SPF environment with an IVC constant temperature and pressure system (20–26 °C, 40–70% humidity, 12-hour light/dark cycle) and provided with autoclaved food and water changed twice a week. The study was reviewed and approved by the Experimental Animal Welfare and Ethics Committee of Shanghai University of Traditional Chinese Medicine (Approval No. PZSHUTCM201204017). QD (30 mg, provided by Putian Delong Pharmaceutical Co., Ltd., Fujian Province, China, GMP drugs, FJ20180005) was administered as the intervention dose, equivalent to 9.1 times the highest clinical dose. The gavage dose for C57 mice was 30 mg/kg, prepared as a suspension of 0.5% sodium carboxymethyl cellulose (CMC) suspension at 3 mg/mL. The 20 mice were randomly divided into two groups: the Control group and the QD group (10 mice per group). Mice in the QD group received 0.2 mL of the QD suspension by gavage daily, while the Control group received the same volume of saline for one week. Four hours after the last gavage, the mice were anesthetized, and 0.5–0.6 mL of blood was drawn by inserting a syringe into the point of strongest heartbeats. The collected blood was left to stand for 30 min and then centrifuged at 3000 rpm for 10–15 min at 4 °C to separate the serum. Serum samples from the mice were placed at 4 °C for 60 min to rehydrate.

Serum samples from both the Control and QD groups were mixed with cold methanol (I1139035113, Merck) at a 1:3 ratio, vortexed for 5 min, and centrifuged (15 min, 12000 rpm, 4 °C). The supernatant was concentrated, dried by centrifugation, and stored at -20 °C. The pre-analytical residue was reconstituted with 100 µl of 50% methanol, vortexed for 5 min, and centrifuged (15 min, 12,000 rpm, 4 °C) to obtain the supernatant.

UPLC-Q-TOF-MS analysis

UPLC-Q-TOF-MS analysis was performed using an Agilent 1290 UPLC system (Agilent Technologies Co., Santa Clara, CA, USA) coupled with an AB SCIEX Triple TOF® 4600 system (AB SCIEX, Foster City, CA, USA). Chromatographic separation was conducted on an Agilent ZORBAX RRHD Eclipse XDB-C18 column (2.1×100 mm, 1.8 µm) at 30 °C employing a mobile phase consisting of 0.1% formic acid in water (mobile phase A) and 0.1% formic acid in acetonitrile (mobile phase B). The gradient elution program used was as follows: 0–5 min, 5% B; 5–10 min, 5–30% B; 10–20 min, 30–60% B; 20–38 min, 60–95% B; 38–42 min, 95–95% B. The flow rate was 0.3 mL/min, and the sample injection volume was 1 µL. Data acquisition was performed on an AB SCIEX Triple TOF® 4600 system equipped with an electrospray ionization (ESI) source in positive and negative ion modes. The mass spectrometer operated in full-scan TOF-MS at m/z 50-1700 with information-dependent acquisition (IDA) MS/MS modes. The mass spectrometry parameters were as follows: ion source gas 1 and 2 at 50 psi; curtain gas at 35 psi; ion source temperature at 500 °C; ion spray voltage floating at 5000 V (positive)/4500 V (negative). Tandem mass spectrometry (MS/MS) experiments featured a mass range of 50-1250, collision energy at 40±20 eV, ion release delay at 30 ms, and ion release width at 15 ms. Data acquisition and processing were validated using Analyst TF 1.7.1. software (AB SCIEX, Foster City, CA, USA).

Network pharmacological analysis

To identify targets associated with the components of QD, firstly, we imported QD components into the PubChem platform (https://pubchem.ncbi.nlm.nih.gov/) to obtain their small molecule structural information numbers (Canonical SMILES) and downloaded their 2D molecular structure SDF files. Subsequently, these molecular structures into two online databases, Similarity Sensitive Approach (http://sea.bkslab.org/) [22], and the PharmaMapper platform (http://lilabecust.cn/pharmmapper/) [23], respectively, for target identification. The Traditional Chinese Medicine System Pharmacology Database and Analysis (TCMSP, http://tcmspw.com/tcmsp.php) [24] was also consulted to obtain additional targets. After eliminating duplicates, the action targets of QD components were determined.

For disease targets related to Ulcerative Colitis (UC), searches were conducted in the DisGeNET database (http://www.disgenet.org/web/DisGeNET/menu/home) [25], DrugBank database (https://www.drugbank.ca/) [26], and TTD database (https://db.idrblab.org/ttd/) [27]. Duplicate disease targets were removed to establish a comprehensive database of UC-related targets. The active targets of QD components were then cross-referenced with UC disease targets to derive QD-UC composite targets. Venn diagrams were generated using Venny 2.1 (https://bioinfogp.cnb.csic.es/tools/venny/index.htm) to visualize the overlap.

In case of an extensive list of composite targets, filtering was performed based on network topology principles. The "Herbs-Ingredients-Targets" network (H-C-T network) was constructed using Cytoscape 3.6.1. Finally, Gene Symbol were converted to Gene_stable_ID using the "Gene ID conversion" tool on OmicShare platform (https://www.omshaire.com/). KEGG enrichment analysis and mapping were performed with the "KEGG Advanced Network Graph" tool to obtain the composite targets for further study.

In vivo study

Mice and ulcerative colitis model establishment

Sixty male C57BL/6 mice were purchased from Shanghai Xipur-Bikai Experimental Animal Co., Ltd (Shanghai, China) and this study protocol was approved by the Experimental Animal Welfare and Ethics Committee of Shanghai University of Traditional Chinese Medicine and adhered to relevant laws and regulations governing animal welfare ethics (ethics clearance number: PZSHUTCM201204017). The mice were housed in a controlled environment (temperature: 23±2 °C; relative humidity: 60±5%; 12-hour light/dark cycle with lights on at 07:00) with ad libitum access to food and water. After one-week adaptation, ten mice were randomly selected as the control group, and the remaining 50 mice were treated with intragastric 3% DSS in distilled water for 10 days to establish an acute UC model. During the 10-day DSS treatment, the mice were randomly divided into six groups with ten mice each and were given the following intragastric administrations once daily: control group (0.2mL saline/day), model group (0.2mL saline/day), QD group (600 mg/kg/day), Indigo group (300 mg/kg/day, Nature Standard, RS01501020), Indirubin group (10 mg/kg/day, Nature Standard, RS01511020), and Tryptophan group (300 mg/kg/day, Alladin, I302392). The mice were observed daily for relative body weight, perianal condition, disease activity index (DAI) score, and survival rate. After ten days of administration, the mice were

euthanized by intraperitoneal injection of pentobarbital sodium.

Anti-UC effects evaluation of QD

The colon tissues of mice from each experimental group were extracted and subjected to hematoxylin-eosin (H&E) and periodic acid-Schiff (PAS) staining. Evaluation of colon integrity, alterations in colonic recesses, inflammatory cell infiltration, distribution, and number of goblet cells were conducted and documented using an Eclipse Ci-L optical microscope (Nikon, Tokyo, Japan). The histopathological evaluation of the colon was quantified using the Tissue Damage Index (TDI).

Total colonic RNA was extracted from individual mice using Trizol reagent (Invitrogen, USA) and reverse transcribed into cDNA using a reverse transcription kit (Takara Bio, Japan). Primers targeting AHR, CYP1A1, RORγt, Foxp3, and GAPDH were synthesized by Sangon Biotech Co. Ltd. (Shanghai, China) (Table S2). The relative expression of target mRNA was calculated using the 2- ΔΔCt method and normalized to GAPDH. Protein bands of AHR, CYP1A1, RORγt, Foxp3, and GAPDH in colon tissues were detected using an electrochemiluminescence (ECL) western blot system (Tanon 4200SF, Shanghai, China). The relative expression levels of these proteins were determined using ImageJ software (Massachusetts, USA) with GAPDH as the internal control.

The expression levels of IL-6, IL-10, IL-17 A, and TGFβ1 in the colon were determined using an ELISA kit (Mlbio, China) according to the manufacturer's protocol. Absorbance was measured at 450 nm, and the resulting concentration was adjusted according to the dilution fold.

Flow cytometry analysis of lamina propria mononuclear cells (LPMCs) in colon tissues

Lamina propria mononuclear cells (LPMCs) were isolated from fresh colon tissues using a previously described method (Yao et al., 2016). Briefly, the colon tissues were incubated in D-Hank's balanced salt solution to eliminate mucus. Epithelial cells were removed using 0.5 mmol/L ethylenediaminetetraacetic acid (EDTA, Seedior, CN) at 37 °C for 30 min. Subsequently, the mucosa was incubated in an enzyme solution (1 mg/mL Collagenase II, 0.01% DNase I, and 25 mmol/L HEPES) at 37 °C for 3–4 h. After passing through a 70 µm cell strainer (BD Falcon, USA), the cells were resuspended in 4 mL of 40% Percoll (Cytiva, CN) and layered over a 70% Percoll solution. The cells at the interface were collected, washed with PBS, and LPMCs were isolated by centrifugation at 1500 rpm for 8 min. The samples were stained and subjected to flow cytometry analysis to detect the ratio of Th17 (CD4+and IL-17 A+) and Treg (CD4+, CD25+, and Foxp3+) cells.

Statistical analysis

Statistical analysis was performed using IBM SPSS Statistics 26.0 and GraphPad Prism 9.0 software. Data were expressed as mean±standard deviation (SD) or ratio. Differences between two groups were assessed using independent t-test or chi- square test, while one-way analysis of variance (ANOVA) was employed for comparisons among multiple groups. Statistical significance was set at $p < 0.05$.

Results

Patients' clinical characteristics at baseline

To study the efficacy of QD in the clinical treatment of UC, A total of 62 patients with UC were included in this study, with 32 in the QD group and 30 in the ADS group. The mean age of patients in the QD group was 39.7 years old, and that in the ADS group was 38.9 years old. The mean duration of disease was 2.55 years in the QD group and 2.32 years in the ADS group. Therefore, there were no significant differences in age and duration of disease between the two groups (all *P* values > 0.05). The extent of the disease and disease activity of UC patients were not significantly different between the two groups (all *P* values > 0.05). And the results showed that QD has a good effect on UC.

Additionally, the scores (MMS, partial Mayo, MMES, and SIBDQ scores) and blood indicators (CRP and ESR) were compared between the QD group and ADS group, and no statistically significant differences were found between the two groups (all *P* values > 0.05). The demographic and clinical characteristics of the two groups at baseline are shown in Table 1. The results further proved that the efficacy of QD in the treatment of UC is equivalent to ADS, demonstrating that QD is an effective treatment option for UC.

QD restores intestinal mucosa in UC patients with comparable efficacy to ADS

In order to observe the recovery of UC patients after QD, this study evaluated the efficacy of QD for UC by observing the mucosal healing of patients. The results showed that the mucosal healing rate of QD group and ADS group at week 16 were 78.13% (25/32) and 60.00% (18/30), respectively. However, there was no statistically significant difference between the two groups (*P*=0.122). The endoscopic response rate at week 16 was similar in both groups (90.63% in the QD group and 80.00% in the ADS group, *P* value=0.235). Additionally, there was no significant difference in clinical remission rate between the two groups (78.13% in the QD group and 56.67% in the ADS group, *P* value=0.071) (Fig. 1 & Table 2). Examples of clinical endoscopy before and after QD treatment are shown in Figure S4. And the results indicated that QD could achieve therapeutic effect by restoring

Table 1 Demographic and baseline clinical characteristics of patients (means ± SD)

Characteristics	QD(*n* = 32)	ADS(*n* = 30)	*P* value [†]
Age (y)	39.7 ± 13.6	38.9 ± 13.5	0.819
Male gender (%)	25 (78.13)	26 (86.67)	0.379
Duration of disease (y)	2.55 ± 2.86	2.32 ± 1.82	0.064
Extent of the disease (%) **(Montreal type)**			
Ulcerative proctitis (E1)	9 (28.13)	10 (33.33)	0.906
Left-sided UC (E2)	16 (50.00)	14 (46.67)	
Extensive UC (E3)	7 (21.88)	6 (20.00)	
Disease activity (%) **(MMS)**			
Mild	5 (15.63)	6 (20.00)	0.652
Moderate	27 (84.37)	24 (80.00)	
MMS	7.69 ± 1.84	7.20 ± 1.77	0.211
Partial Mayo score	3.69 ± 1.03	3.37 ± 0.96	0.448
MMES	2.30 ± 0.53	2.40 ± 0.50	0.695
SIBDQ score	46.93 ± 9.33	49.43 ± 9.17	0.292
Blood indicators			
CRP (mg/L)	9.98 ± 14.44	8.98 ± 14.69	0.648
ESR (mm/h)	18.61 ± 18.73	16.83 ± 16.86	0.644
Hb (g/L)	109.9 ± 15.32	110.5 ± 15.87	0.936
ALB (g/L)	38.70 ± 7.05	38.44 ± 7.55	0.952

[†] *P* values for continuous variables are based on t-test or adjusted t-test. *P* values for all categorical variables are based on a two-sided chi-square test

Table 2 Percentage differences in primary and main secondary efficacy endpoints between QD group and ADS group at 16-week

Outcome (%)	QD (*n* = 32)	ADS (*n* = 30)	Difference (95% CI)	*P* value[†]
Mucosal healing	25(78.13)	18(60.00)	18.13 (-6.9, 40.77)	0.122
Endoscopic response	29(90.63)	24(80.00)	10.63 (-9.78, 30.97)	0.235
Clinical remission	25(78.13)	17(56.67)	21.46 (-3.96, 43.90)	0.071

[†]*P* values for all categorical variables are based on a two-sided chi-square test

Table 3 Difference in means of secondary endpoints between QD group and ADS group at 16-week

Outcome (mean ± SD)	QD (*n* = 32)	ADS (*n* = 30)	*P* value[†]
MMS	2.25 ± 0.51	2.53 ± 0.68	0.070
Partial Mayo score	0.03 ± 0.18	0.13 ± 0.35	0.155
MMES	1.23 ± 0.43	1.40 ± 0.50	0.128
0 (%)	2 (6.25)	2 (6.67)	0.181
1 (%)	23 (71.88)	15 (50.00)	
2 (%)	7 (21.88)	13 (43.33)	
SIBDQ score	67.44 ± 2.34	64.10 ± 5.34	**0.003**
Blood indicators			
CRP (mg/L)	8.19 ± 5.94	8.48 ± 4.42	0.893
ESR (mm/h)	0.88 ± 0.93	0.95 ± 1.48	0.842
Hb (g/L)	124.3 ± 8.92	119.2 ± 8.13	0.198
ALB (g/L)	43.79 ± 3.58	42.03 ± 3.80	0.391

[†]*P* values for continuous variables are based on t-test or adjusted t-test. *P* values for all categorical variables are based on a two-sided chi-square test.* *P* value < 0.05

the intestinal mucosa of UC patients. Table 3 shows the mean and mean differences of MMS, partial Mayo score, MMES, SIBDQ score, ESR level, and CRP level in patients who received QD and ADS at 16 weeks. Compared with patients who received ADS, patients who received QD exhibited greater improvement in SIBDQ score, although there was no significant difference in MMS, partial Mayo
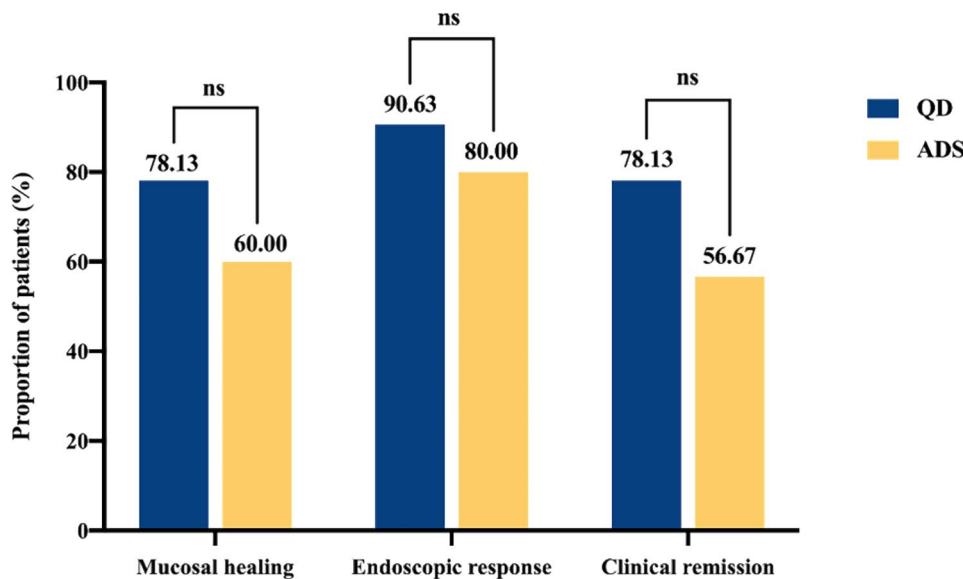

Fig. 1 Proportion of patients in the ADS and QD groups who achieved mucosal healing, endoscopic response, and clinical remission at 16-week. (ns = no significant difference between two groups)
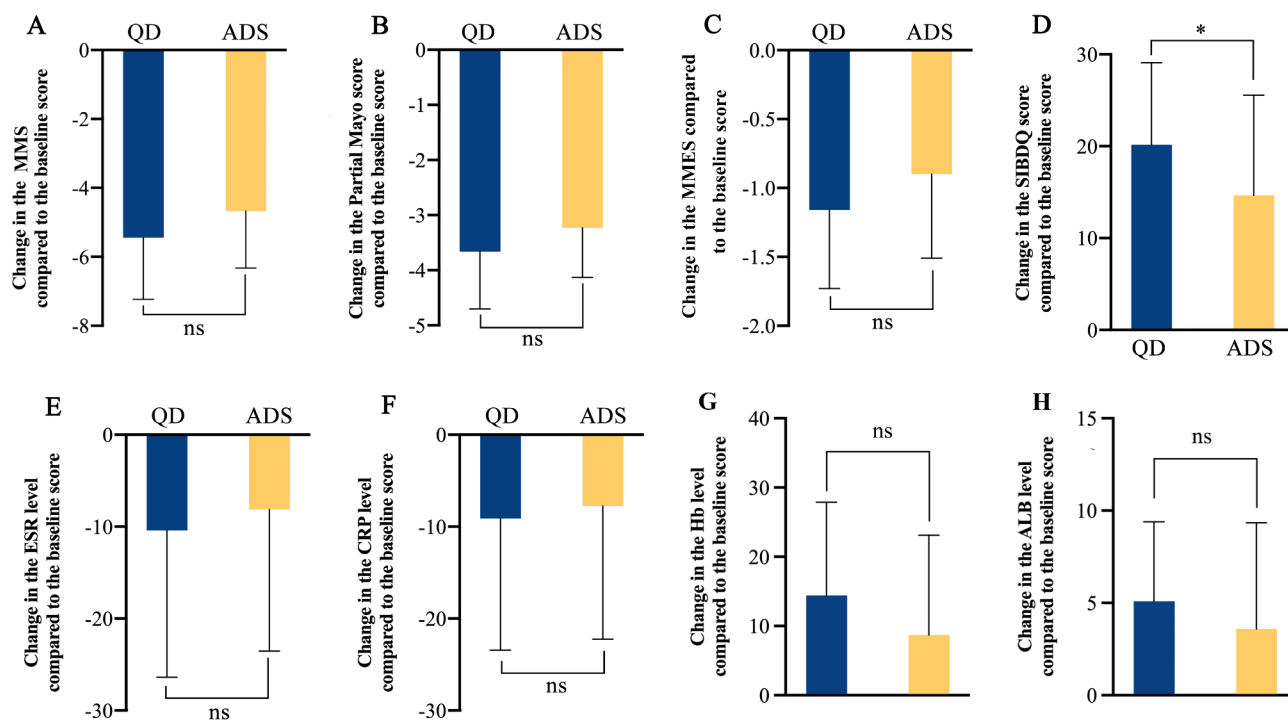
Fig. 2 Changes in the MMS (**A**), Partial Mayo score (**B**), MMES (**C**), SIBDQ score (**D**), ESR level (**E**), CRP level (**F**), Hb level (**G**) and ALB level (**H**) from baseline to week 16. Results are expressed as mean ± SD.*P value < 0.05

Table 4 Summary of adverse events and outcomes in QD and ADS groups

	QD ($n = 32$)		ADS ($n = 30$)	
	All events	Therapy-related events	All events	Therapy-related events
No. of adverse events	5(15.6%)	4(12.5%)	7(23.3%)	4(13.3%)
Serious adverse events	0	0	0	0
Adverse events				
Liver dysfunction	0	2(6.2%)	1(3.3%)	1(3.3%)
Epigastric pain/abdominal pain	0	2(6.2%)	1(3.3%)	1(3.3%)
Leukopenia	1(3.1%)	0	0	1(3.3%)
Elevated amylase	0	0	1(3.3%)	1(3.3%)

score, and MMES (Fig. 2 & Table S3). Additionally, there was no significant difference in ESR, CRP, Hb and ALB levels between the two groups (Fig. 2 & Table S3).

Adverse event comparison between QD and ADS groups
In this study, the incidence of adverse events in the QD group and ADS group was 15.6% (5 cases) and 23.3% (7 cases), respectively, with therapy-related adverse events occurring in 12.5% (4 cases) and 13.3% (4 cases). No serious adverse events were reported in either group (Table 4). Two patients in both the QD and ADS groups experienced mild liver dysfunction, with transaminase levels returning to normal after the study in the QD

group, while spontaneous recovery occurred in the ADS group. One case of leukopenia in the QD group resolved spontaneously, and in the ADS group, leukopenia resolved after the study. Additionally, two patients with elevated amylase in the ADS group also experienced spontaneous recovery.

Identification of active components in QD for UC treatment using UPLC-Q-TOF/MS
To further investigate the potential active components of QD in treating UC, this study first used UPLC-Q-TOF/MS to analyze serum samples from UC patients before and after QD administration. However, the results showed that no QD-related components were detected in the patient blood samples 4 h after administration (Figure S5). Therefore, we subsequently performed UPLC-Q-TOF/MS analysis on the exogenous components in the serum of mice after QD administration. By comparing mass spectrometry fragments and matching with the Natural Products HR-MS/MS Spectral Library 1.0, a total of 16 components were identified from the serum of QD-treated mice [28]. Among the identified components were 8 prototype compounds—indigo, indirubin, tryptanthrin, quindoline, Bisindigotin, 1 H-indole-3-aldehyde, 3-(2-carboxyphenyl)-4(3 H)-quinazolinone, and 2-[cyano(3-indolyl)methylene]-3-indolone—as well as 8 metabolites, including phenyl carbonimide, tryptophan + hydroxylation, Indirubin isomer indirubin + dihydroxylation, indirubin + hydroxylation + hydrogenation,

Gu *et al. Journal of Inflammation*   (2024) 21:44

Page 8 of 14

indirubin+hydroxylation, tryptophan+hydroxylation, and indirubin+hydroxylation+hydrogenation (Table 5).

Network Pharmacology reveals the mechanism of QD in treating UC

To further investigate the active ingredients and targets of QD in treating UC, this study employed a network pharmacology approach to construct a "compound-target-disease" network, identifying the active components and targets of QD in UC treatment (Fig. 3A). First, the targets of 16 QD components were individually retrieved from the TCMSP database, and only 3 components (indirubin, indigo, and quindoline) yielded a total of 69 targets. Subsequently, the 16 compounds were imported into the PubChem database, which identified 7 compounds with their corresponding Canonical SMILES numbers and molecular structures. These 7 compounds were then imported into the SEA and PharmMapper databases for target fishing. After combining with the targets obtained from TCMSP and removing duplicates, a total of 490 unique targets were identified (Table S4). A total of 962 UC disease targets were obtained by searching the DisGeNET, DrugBank, and TTD databases.

The target of QD was matched with UC disease target, and 67 QD-UC compound targets were obtained (Fig. 3B). The network diagram of QD component targets-UC composite targets was constructed (Fig. 3C). According to the KEGG enrichment analysis results on the OmicShare platform, we determined that the main signaling pathways involved in the combination target of QD-UC include the TNF signaling pathway (ko04668), IL-17 signaling pathway (ko04657), Toll-like receptor signaling pathway (ko04620), Th17 cell differentiation (ko04659), Th1 and Th2 cell differentiation (ko04658), VEGF signaling pathway (ko04370), and others. 20 UC-related signaling pathways were selected to construct the "Compounds target-signaling pathway" network diagram (Fig. 3D). And it could be inferred that the treatment of UC with QD involves a multifaceted and multitargeted mechanism, where multiple components and targets collaborate to exert therapeutic effects on UC.

Active components of QD alleviate UC by promoting Colon recovery and increasing goblet cells

By combining UPLC-Q-TOF/MS and network pharmacology analysis, this study identified indigo, indirubin, and tryptanthrin as potential active components for treating UC, and assessed their therapeutic effects in a UC model. Compared to the control group, the model group exhibited significant body weight loss, an elevated DAI score, and a marked shortening of colon length. After intervention, significant increases in body weight were observed only in the QD, indigo, and indirubin groups, while all intervention groups (QD, indigo, indirubin, and tryptanthrin) showed significant decreases in DAI scores and increases in colon length (all P values<0.05, Fig. 4A-D).

Pathological observations of HE staining in the model group revealed obvious damage to the mucosal structure of colonic tissue, the absence of colonic recess, mucosal erosion, and infiltration of significant neutrophils and lymphocytes in the mucosa and submucosa. Moreover, the TDI scores were significantly higher (P value<0.05). Conversely, the histological colonic damage was significantly alleviated, and the TDI scores were significantly lower in the QD and its components groups than the model group (P value<0.05) (Fig. 4E).

The number of goblet cells in each group was observed by PAS staining. Compared to the control group, the

Table 5 Main components of QD in mouse serum

| No.	Compound	Molecular formula	Molecular weight	Retention time (min)
1	Phenyl carbonimide	C_7H_5NO	119.04	8.62
2	Tryptanthrin+hydroxylation	$C_{15}H_8N_2O_3$	264.05	11.18
3	Indirubin isomer	$C_{16}H_{10}N_2O_2$	262.07	12.19
4	Indirubin+Dihydroxylation	$C_{16}H_{10}N_2O_4$	294.06	12.53
5	Indirubin+hydroxylation+hydrogenation	$C_{16}H_{12}N_2O_3$	280.08	13.55
6	Indirubin+hydroxylation	$C_{16}H_{10}N_2O_3$	278.07	13.99
7	Tryptanthrin+hydroxylation	$C_{15}H_8N_2O_3$	264.05	15.75
8	Indirubin+hydroxylation+hydrogenation	$C_{16}H_{12}N_2O_3$	280.08	15.81
9	Quindoline	$C_{15}H_{10}N_2$	218.08	11.01
10	1 H-indole-3-aldehyde	C_9H_7NO	145.05	11.01
11	3-(2-Carboxyphenyl)-4(3 H)-quinazolinone	$C_{15}H_{10}N_2O_3$	266.07	11.63
12	Tryptanthrin	$C_{15}H_8N_2O_2$	248.06	16.05
13	Indigo	$C_{16}H_{10}N_2O_2$	262.07	17.79
14	Indirubin	$C_{16}H_{10}N_2O_2$	262.07	18.63
15	2-[Cyano(3-indolyl)methylene]-3-indolone	$C_{18}H_{11}N_3O$	285.09	19.79
16	Bisindigotin	$C_{32}H_{18}N_4O_2$	490.14	27.27
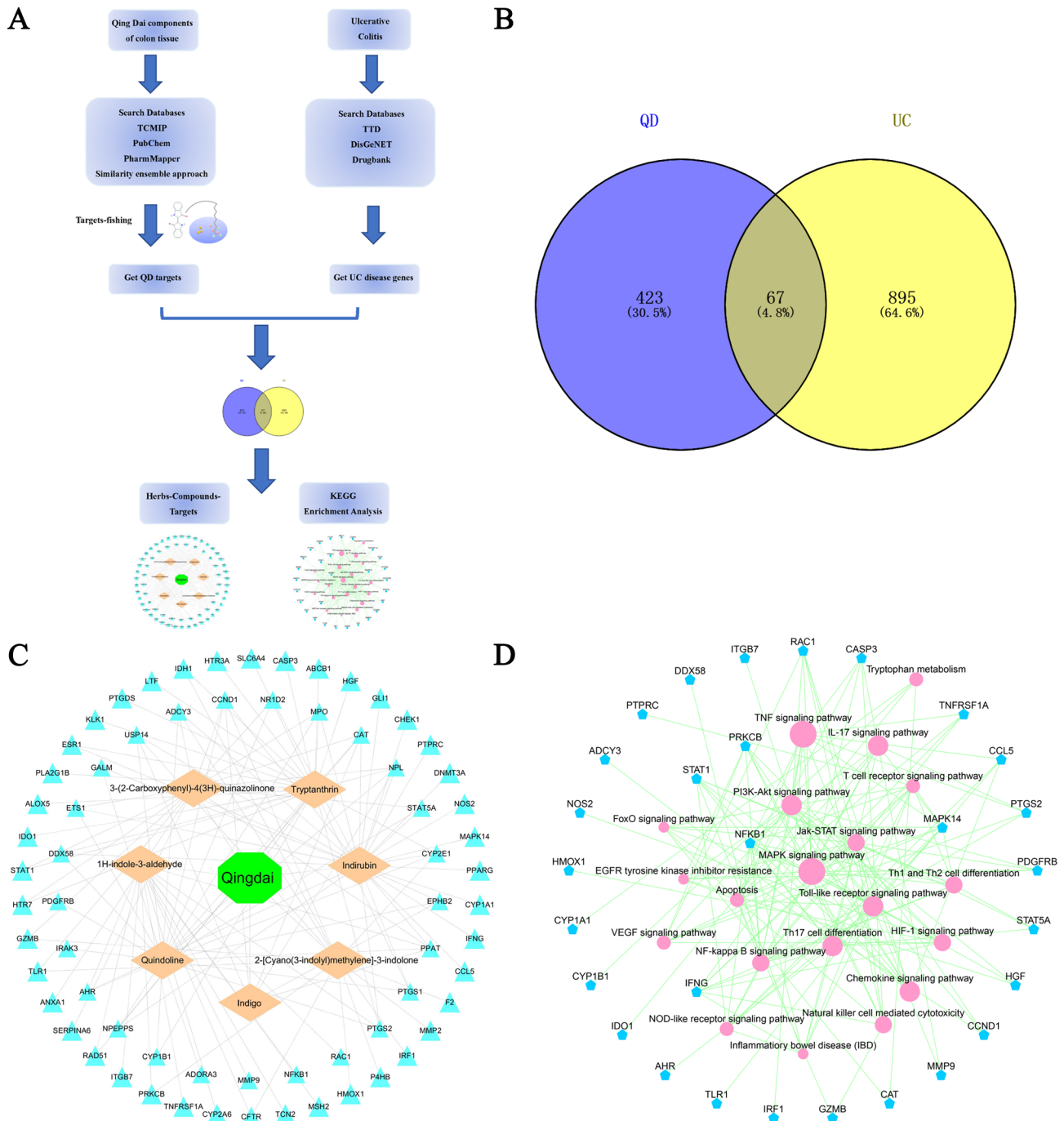
Fig. 3 Network Pharmacology of QD. (**A**) Flow chart of Network Pharmacology. (**B**) Venn diagram of QD component targets and UC disease targets. (**C**) QD component targets-UC Composite targets network diagram. (**D**) Composite targets-Core UC related signal pathways network diagram

number of goblet cells per unit length of the intestinal gland epithelium in the model group basically disappeared (*P*value<0.05). In contrast, after treatment with QD and its components, the number of goblet cells increased significantly compared to the model group (*P*value<0.05). These results suggest that the active components of QD may treat UC by promoting colon

lengthening, reducing colon damage, and increasing goblet cell numbers (Fig. 4F).

Regulation of treg and Th17 cells in colon tissue by QD and its active components via the AHR pathway

For investigate whether QD and its active components could affect Treg and Th17 cells in colon tissue through the aromatic hydrocarbon receptor (AHR), mRNA
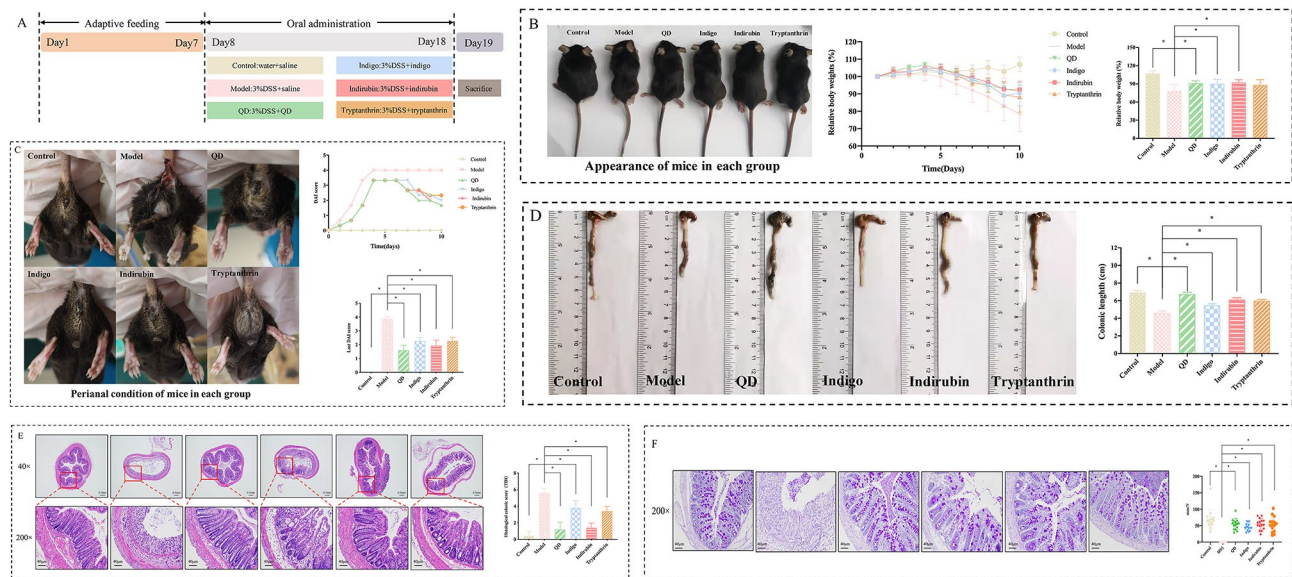
Fig. 4 Effects of QD and its active components administration on UC mice (*n* = 5). (A) The protocol of UC modeling and intervention. (B) Appearance and relative changes of body weight in each group. (C) Perianal condition and changes of DAI score in each group. (D) Length of colon in each group. (E) The pathological observation (H&E staining) and TDI score in each group. (F) The pathological observation (PAS staining) and the number of goblet cells. (∗*P* value < 0.05)
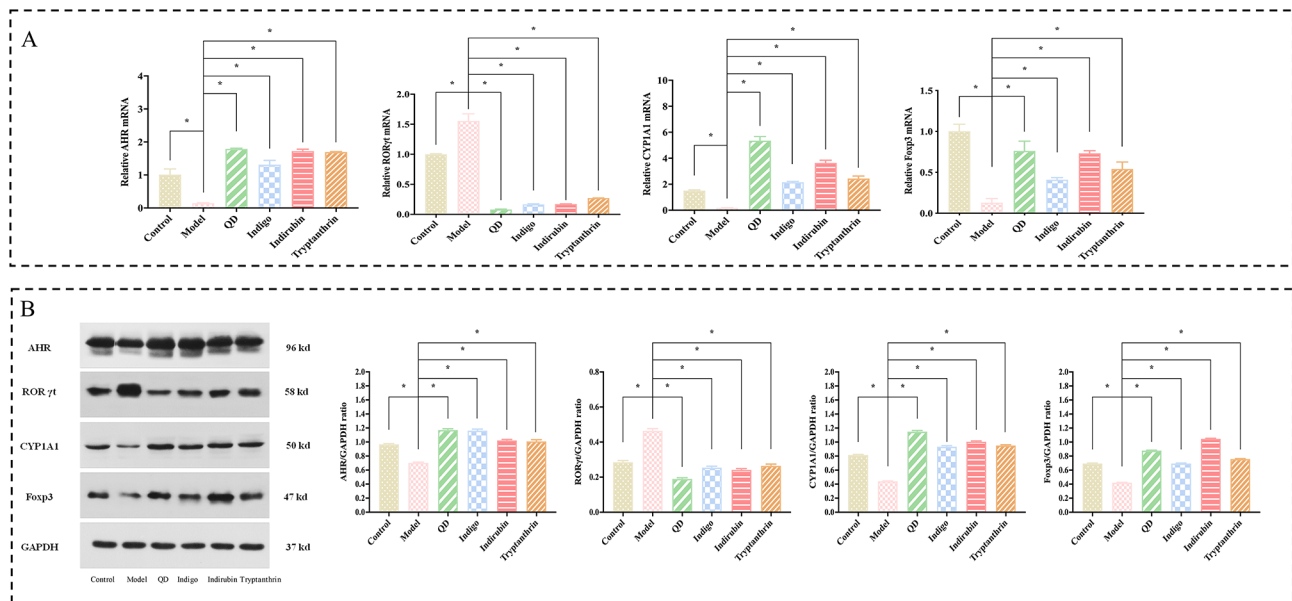

Fig. 5 QD and its active components might affect Treg and Th17 cells in colon tissues of mice through AHR activation (*n* = 5). (**A**) The mRNA levels of AHR, RORγt, CYP1A1 and Foxp3 in each group. (**B**) The protein levels of AHR, RORγt, CYP1A1 and Foxp3 in each group. (∗*P* value < 0.05)

and protein expressions of AHR and the marker gene for AHR activation (CYP1A1), Treg (Foxp3) and Th17 (RORγt) were analyzed, respectively.

After DSS induction, mRNA and protein levels of AHR, CYP1A1, and Foxp3 in the colon tissue of mice in the model group decreased significantly (all *P* values < 0.05) (Fig. 5). Conversely, mRNA and protein levels of RORγt increased significantly (*P* value < 0.05) (Fig. 5). Moreover, after the intervention of QD and its active components,

mRNA and protein levels of AHR, CYP1A1, and Foxp3 in the colon tissue of mice were significantly increased (all *P* values < 0.05) (Fig. 5), while mRNA and protein levels of RORγt decreased significantly (*P* value < 0.05) (Fig. 5). The results further demonstrate that components in QD exert therapeutic effects on the UC model mice by upregulating the mRNA and protein levels of AHR, CYP1A1, and Foxp3 in colonic tissues, while downregulating the mRNA and protein levels of RORγt.

QD and its active components regulate the balance of CD4+T cell subsets and the expression of related cytokines in UC mice

To evaluate the in vivo effects of QD and its active components on CD4+T cells in UC mice, we determined the frequencies of CD4+CD25+Foxp3+ (Treg) and CD4+IL-17 A+ (Th17) cells in the LPMCs of DSS-induced mice after different drug interventions. The frequency ratio of Treg/Th17 (an indicator to assess the Treg/Th17 balance) in LPMCs of the model group decreased significantly (P value < 0.05) (Fig. 6A), while QD and its active components significantly increased the frequency ratio of Treg/Th17 (P value < 0.05): the frequency of Treg cells increased and the frequencies of Th17 cells decreased (all P values < 0.05) (Fig. 6A). Furthermore, the ELISA results confirmed that QD and indirubin also increased the concentrations of Treg-associated cytokines (IL-10 and TGFβ1) and decreased those
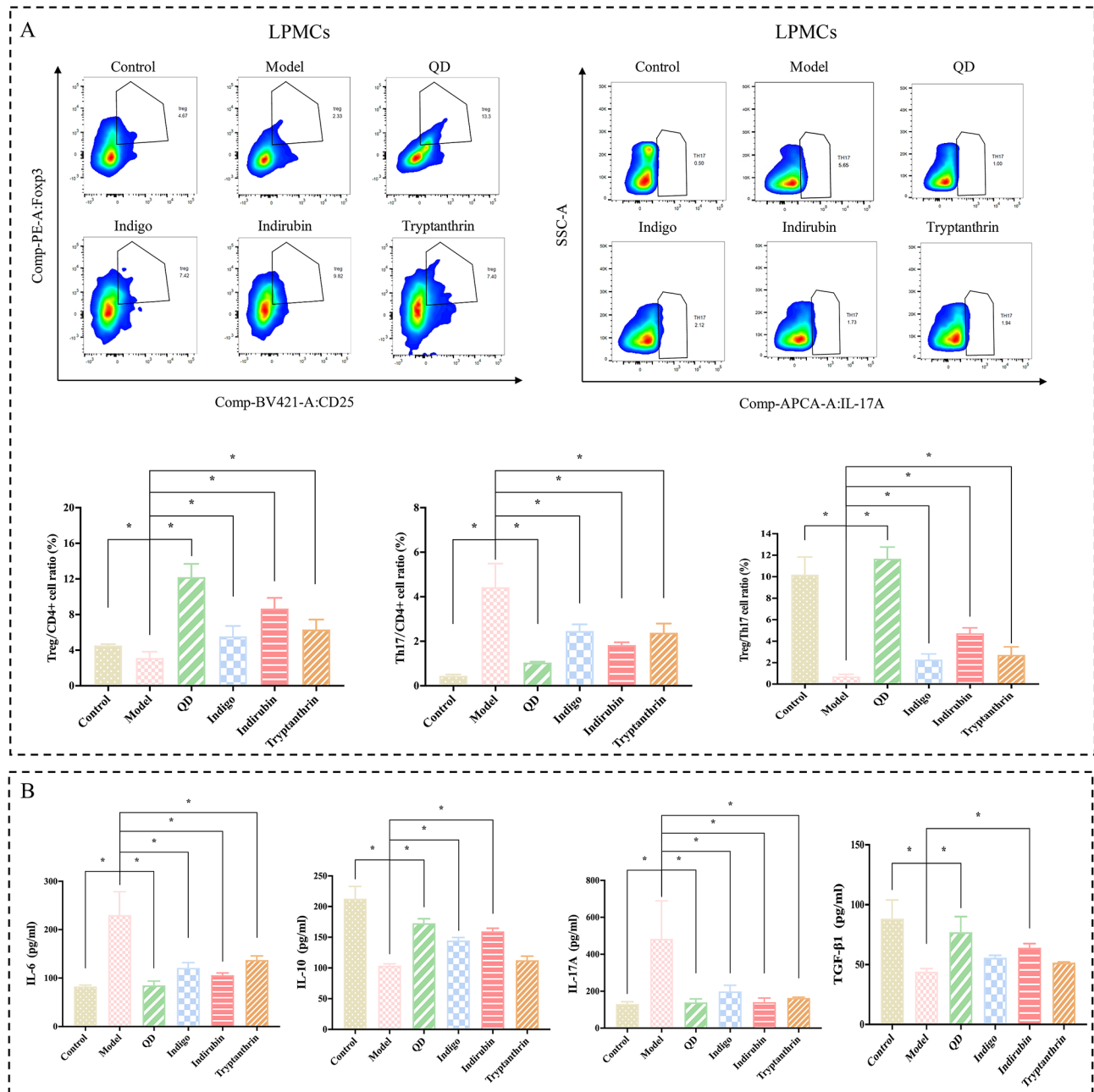

Fig. 6 QD and its active components shifted Th17 dominance to Treg dominance in UC mouse (n = 5). (**A**) Representative frequencies of CD4 + Foxp3 + cells (Treg) and CD4 + IL-17+ (Th17) cells were presented in LPMCs of mice and the frequency ratios of Treg/Th17 were compared in each group. (**B**) The concentrations of Treg and Th17 lineage-associated cytokines (IL-6, IL-10, IL-17 A and TGFβ1) were presented in serum samples of mice in each group. (∗P value < 0.05)

of Th17- associated cytokines (IL-6 and IL-17 A) in the colon of mice (all *P* value < 0.05) (Fig. 6B).

Discussion

UC is a persistent and challenging intestinal disease globally, with significant obstacles to mucosal repair. Achieving mucosal healing has become a key goal in UC treatment, serving as a critical indicator for maintaining remission, reducing relapse and complications, lowering hospitalization and surgery rates, and improving the quality of life for UC patients. Despite the widespread use of traditional therapeutic drugs, some UC patients remain unresponsive, highlighting the need for more effective treatment options.

In this study, we conducted a 16-week observation on Chinese patients with mild to moderate active UC, assessing the efficacy of QD capsules as a potential first-line treatment. Our findings showed that the mucosal healing rate in the QD group was comparable to that in the Adisha group after 16 weeks of treatment. Additionally, analysis of the SIBDQ scores post-treatment revealed a greater improvement in quality of life for the QD group compared to the Adisha group. These results indicate that QD is not only effective, convenient, and economical but also significantly reduces patient anxiety, contributing positively to disease recovery and stability. However, due to the relatively small sample size, future studies should expand the cohort to further validate the efficacy and safety of QD.

Although QD has shown clinical efficacy, its chemical foundation and mechanism of action are not fully understood. In this study, we used liquid chromatography techniques to investigate the pharmacological components of QD in vivo. Utilizing UPLC-Q-TOF-MS and the natural product HR-MS/MS spectral library 1.0 database and standards, we identified 20 alkaloids, 8 fatty acids, and 2 terpenoids, with 7 compounds identified as prototypical, including quindoline, 1 H-indole-3-aldehyde, 3-(2-carboxyphenyl)-4(3 H)-quinazolinone, tryptophan, indirubin, 2-[cyano(3indolyl)methylene]-3-indolone, bisindigotin, and phenyl carbonimide. Furthermore, 9 metabolites were identified, including 6 metabolites or isomers of indirubin and hydroxylated tryptophan. Previous studies suggest that indole alkaloids, which play a crucial role in QD's pharmacological activity, are poorly absorbed due to their low solubility [29]. Indole substances like indirubin [30] and tryptophan [31] rapidly distribute into surrounding tissues, resulting in low plasma levels of prototype components and metabolites. It is believed that indole substances primarily dissolve in bile and are excreted into the intestine along with bile, suggesting that QD may exert its therapeutic effects by permeating local colon tissues and aiding mucosal repair.

The activation of the AHR is a promising avenue for UC treatment [19, 20], with studies showing that AHR plays a vital role in regulating Th17/Treg cell differentiation [18]. A lack of AHR leads to decreased expression of Foxp3 and increased expression of RORγt and IL-17 [32, 33]. Different AHR ligands may have varying effects, with some upregulating Treg differentiation and others exacerbating UC by increasing Th17 cell activity [34]. For instance, indigo and tryptanthrin can dose-dependently inhibit the expression of IL-17 A.

In our study, an acute UC model was established using 3% DSS in drinking water [25]. The results showed that QD, indigo, indirubin, and tryptophan could control weight loss and improve the overall condition of the animals, with the QD and Indirubin groups being the most effective. Histological analysis revealed that the QD group showed the most significant mucosal repair, with improved goblet cell count and reduced inflammatory cell infiltration.

In colonic tissues, QD significantly upregulated AHR, CYP1A1, and Foxp3 mRNA and protein levels, while downregulating RORγt mRNA and protein levels, outperforming the other three components. In LPMCs, QD showed the most significant effect in reducing Th17 cells and increasing Treg cells. The QD and Indirubin groups also significantly decreased IL-6 and IL-17 A levels, and increased TGF-β1 levels, suggesting a strong anti-inflammatory effect.

Overall, these findings suggest that QD and its main components can significantly promote colonic mucosal repair and improve inflammation, with QD showing the most pronounced effects. These results indicate that QD has potential as a therapeutic strategy for UC treatment.

Conclusion

This study comprehensively investigated the active components and therapeutic targets of QD in the treatment of UC, employing a combination of clinical case analysis, serum pharmacological profiling via UPLC-Q-TOF-MS, network pharmacology, and both in vivo and in vitro validations. The findings demonstrate that oral administration of QD capsules effectively induces clinical remission in patients with active UC, with therapeutic outcomes comparable to those of mesalamine granules. The primary active components of QD, identified as indigo, indirubin, and tryptanthrin, play a crucial role in its efficacy against UC. Furthermore, QD and its key components appear to restore the Th17/Treg balance by activating the AHR pathway in the intestinal mucosa, highlighting this mechanism as a pivotal factor in QD's ability to promote colonic mucosal repair in UC patients.

Abbreviations
QD　　　　　　　　Qingdao
UC　　　　　　　　Ulcerative colitis

UPLC-Q-TOF-MS	Ultra-Performance Liquid Chromatography-Quadrupole-Time of Flight-Mass Spectrometry
Treg	Regulatory T cells Th17 helper T cells 17
AHR	Aryl Hydrocarbon Receptor GSC Gastroenterology
ESR	Erythrocyte sedimentation rate CRP C-reactive protein
CMC	Sodium carboxymethyl cellulose PCR Polymerase Chain Reaction
WB	Western Blot
ELISA	Enzyme-linked immunosorbent assay
TCMSP	Traditional Chinese Medicine System Pharmacology Database and Analysis TDI Tissue Damage Index
LPMCs	Lamina propria mononuclear cells
SIBDQ	Short inflammatory bowel disease questionnaire H&E Hematoxylin-eosin
PAS	Periodic acid-Schiff DAI disease activity index
CYP1A1	Cytochrome p450 1A1 Foxp3 Forehead box protein 3
RORγt	Retinoid-related orphan nuclear receptor γt

Supplementary Information

The online version contains supplementary material available at https://doi.org/10.1186/s12950-024-00413-x.

> Supplementary Table S1: Component identification of QD
>
> Supplementary Table S2: The Primer sequence of AHR, CYP1A1, RORγt, Foxp3 and GAPDH
>
> Supplementary Table S3: Difference in the mean changes in secondary endpoints between QD group and ADS group from baseline to week 16
>
> Supplementary Table S4: Functional targets of QD components
>
> Supplementary Figure S1: UPLC-HRMS base peak chromatogram (BPC) of QD. (**A**) Negative ion mode; (**B**) Positive ion mode
>
> Supplementary Figure S2: QD capsule. (**A**) Appearance of QD powder; (**B**) Appearance of the capsule
>
> Supplementary Figure S3: Trial process and patient disposition
>
> Supplementary Figure S4: Clinical endoscopic examples before and after QD treatment of different types of UC (representative 3 cases). (**A**) Type E1 UC; (**B**) Type E2 UC; (**C**) Type E3 UC
>
> Supplementary Figure S5: Serum Concentration Analysis of QD Components in UC Patients

Author contributions

Gu Sizhen and Xue Y contributed equally to this work, and both performed most of the clinical and animal experiments, wrote and revised the paper; Liu Xiaowen were responsible for animal experimental feeding, sampling and data analysis; Tang Yini and Wang Dong collected UC patients and performed colonoscopy assessment before and after treatment; Wu Dongmei, Yao Mingrong, Xia Zehua and Yang sen were responsible for animal pathology, PCR, WB and flow cytometry. Dou DB and Cai G designed and coordinated the research. Xue Shigui and Dou DB are responsible for the paper. The authors declare that all data were generated in-house and that no paper mill was used.

Funding

Data availability

No datasets were generated or analysed during the current study.

Declarations

Conflict of interest

The authors declare no conflicts of interest related to this study.

Author details

[1]Department of Traditional Chinese Medicine, Shuguang Hospital Affiliated to Shanghai University of Traditional Chinese Medicine, Shanghai 201203, P.R. China
[2]Department of Traditional Chinese Medicine, Shanghai Yangzhi Rehabilitation Hospital (Shanghai Sunshine Rehabilitation Centre), China, Shanghai 201619, P.R. China
[3]Department of Digestive Endoscopy Center, Shuguang Hospital Affiliated to Shanghai University of Traditional Chinese Medicine, Shanghai 201203, P.R. China
[4]Department of Gastroenterology, The second hospital of Hebei Medical University, Shijiazhuang City 05000, Hebei Province, P.R. China
[5]Department of Pathology, Shuguang Hospital Affiliated to Shanghai University of Traditional Chinese Medicine, Shanghai 201203, P.R. China
[6]Department of Radiology, Shuguang Hospital Affiliated to Shanghai University of Traditional Chinese Medicine, Shanghai 201203, P.R. China
[7]Department of Anorectal, Shuguang Hospital affiliated to Shanghai University of traditional Chinese Medicine, Shanghai 201203, P.R. China
[8]Department of Clinical Lab, Shuguang Hospital affiliated to Shanghai University of traditional Chinese Medicine, Shanghai 201203, P.R. China
[9]Department of Gastroenterology, Shuguang Hospital Affiliated to Shanghai University of Traditional Chinese Medicine, Shanghai 201203, P.R. China

References

1. Xuefeng L, Xia P, Minghuan Z. Progress in epidemiological research on inflammatory bowel disease in China. Mod Digestion Intervention. 2020;25(09):1265–7.
2. Naganuma M. Treatment with indigo naturalis for inflammatory bowel disease and other immune diseases. Immunol Med. 2019;42(1):16–21.
3. Naganuma M, Mizuno S, Nanki K, Sugimoto S, Kanai T. Recent trends and future directions for the medical treatment of ulcerative colitis. Clin J Gastroenterol. 2016;9(6):329–36.
4. Sandborn WJ, Feagan BG, Marano C, Zhang H, Strauss R, Johanns J, Adedokun OJ, Guzzo C, Colombel JF, Reinisch W, et al. Subcutaneous golimumab induces clinical response and remission in patients with moderate-to-severe ulcerative colitis. Gastroenterology. 2014;146(1):85–95.
5. Qiong L, Zhe C, Guang C. Progress in traditional Chinese medicine treatment of ulcerative colitis. Chin J Basic Med Traditional Chin Med. 2021;27(07):1191–4.
6. male W, Guanhua L. Overview of clinical compatibility and application of Indigo Naturalis in Ancient and Modern Times. Jiangxi Traditional Chin Med. 2018;49(05):74–6.
7. Yang G, Sizhen G, Kanjun C, Shuyang S, Danbo D. Thinking and clinical experience of Dou Danbo's application of Qingyu Powder in the treatment of Ulcerative Colitis. Chin J Traditional Chin Med. 2021;36(09):5311–5.
8. Gong Y, Zha Q, Li L, Liu Y, Yang B, Liu L, Lu A, Lin Y, Jiang M. Efficacy and safety of Fufangkushen colon-coated capsule in the treatment of ulcerative colitis compared with mesalazine: a double-blinded and randomized study. J Ethnopharmacol. 2012;141(2):592–8.
9. Mingshi C, Liyang D, Jie Z. Observation on the efficacy of compound Qingdai granules combined with probiotics in the treatment of ulcerative colitis. Chin J Integr Traditional Western Med Digestion. 2017;25(10):751–4.
10. Yi Z. Observation on the therapeutic effect of Qingdai powder on ulcerative colitis. J Mod Integr Traditional Chin Western Med. 2016;25(29):3238–40.
11. Zhibin W, Chen C, Yi G, Lei S, Zhongmei S, Tangyou M, Xiaowei C, Junxiang L. Clinical study on Qingchang Wenfang decoction in the treatment of mild to

moderate ulcerative colitis. Chin J Integr Traditional Western Med Digestion. 2018;38(01):15–9.

12. Sugimoto S, Naganuma M, Kiyohara H, Arai M, Ono K, Mori K, Saigusa K, Nanki K, Takeshita K, Takeshita T, et al. Clinical efficacy and safety of oral Qing-Dai in patients with Ulcerative Colitis: a single-center open-label prospective study. Digestion. 2016;93(3):193–201.

13. Naganuma M, Sugimoto S, Mitsuyama K, Kobayashi T, Yoshimura N, Ohi H, Tanaka S, Andoh A, Ohmiya N, Saigusa K, et al. Efficacy of Indigo Naturalis in a Multicenter Randomized Controlled Trial of patients with Ulcerative Colitis. Gastroenterology. 2018;154(4):935–47.

14. Suzuki H, Kaneko T, Mizokami Y, Narasaka T, Endo S, Matsui H, Yanaka A, Hirayama A, Hyodo I. Therapeutic efficacy of the Qing Dai in patients with intractable ulcerative colitis. World J Gastroenterol. 2013;19(17):2718–22.

15. Sugimoto S, Naganuma M, Kanai T. Indole compounds may be promising medicines for ulcerative colitis. J Gastroenterol. 2016;51(9):853–61.

16. Gu S, Xue Y, Gao Y, Shen S, Zhang Y, Chen K, Xue S, Pan J, Tang Y, Zhu H, et al. Mechanisms of indigo naturalis on treating ulcerative colitis explored by GEO gene chips combined with network pharmacology and molecular docking. Sci Rep. 2020;10(1):15204.

17. Sherr D, Monti S. The role of the aryl hydrocarbon receptor in normal and malignant B cell development. Semin Immunopathol. 2013;35(6):705–16.

18. Liangzi L, Zhongze L, Weigang C, Hua Y. Study on the Alleviative Effect and Mechanism of Aromatic Hydrocarbon Receptors on colitis in mice. J Immunol. 2017;33(01):13–7.

19. Monteleone I, Rizzo A, Sarra M, Sica G, Sileri P, Biancone L, MacDonald TT, Pallone F, Monteleone G. Aryl hydrocarbon receptor-induced signals up-regulate IL-22 production and inhibit inflammation in the gastrointestinal tract. Gastroenterology. 2011;141(1):237–48. 248 e231.

20. Wang C, Ye Z, Kijlstra A, Zhou Y, Yang P. Activation of the aryl hydrocarbon receptor affects activation and function of human monocyte-derived dendritic cells. Clin Exp Immunol. 2014;177(2):521–30.

21. Peirong L, Rong P, Zhiping W, Dekui Z. The role and research progress of Th17/Treg cells and their related cytokines in the pathogenesis of ulcerative colitis. World Sci Technological Res Dev. 2017;39(02):194–7.

22. Keiser MJ, Roth BL, Armbruster BN, Ernsberger P, Irwin JJ, Shoichet BK. Relating protein pharmacology by ligand chemistry. Nat Biotechnol. 2007;25(2):197–206.

23. X W, W Z YSSWSL. PharmMapper 2017 update: a web server for potential drug target identification with a comprehensive target pharmacophore database. Nucleic Acids Res. 2017;45:W356–60.

24. C JRPLJWWZBL, Z HPL, W G. TCMSP: a database of systems pharmacology for drug discovery from herbal medicines. J Cheminform. 2014;6:13.

25. Kawai S, Iijima H, Shinzaki S, Hiyama S, Yamaguchi T, Araki M, Iwatani S, Shiraishi E, Mukai A, Inoue T, et al. Indigo Naturalis ameliorates murine dextran sodium sulfate-induced colitis via aryl hydrocarbon receptor activation. J Gastroenterol. 2017;52(8):904–19.

26. Wishart DS, Feunang YD, Guo AC, Lo EJ, Marcu A, Grant JR, Sajed T, Johnson D, Li C, Sayeeda Z, et al. DrugBank 5.0: a major update to the DrugBank database for 2018. Nucleic Acids Res. 2018;46(D1):D1074–82.

27. YH L, CY Y, Q XXLPZJT. Therapeutic target database update 2018: enriched resource for facilitating bench-to-clinic research of targeted therapeutics. Nucleic Acids Res. 2018;46:D1121–7.

28. Hao Y, Huo J, Wang T, Sun G, Wang W. Chemical profiling of Coptis rootlet and screening of its bioactive compounds in inhibiting Staphylococcus aureus by UPLC-Q-TOF/MS. J Pharm Biomed Anal. 2020;180:113089.

29. Sun Q, Leng J, Tang L, Wang L, Fu C. A Comprehensive Review of the Chemistry, Pharmacokinetics, Pharmacology, clinical applications, adverse events, and Quality Control of Indigo Naturalis. Front Pharmacol. 2021;12:664022.

30. Kejia L. Study on the oral absorption mechanism of indirubin. Master. Sichuan University; 2007.

31. Jie L, Shan M, Siwang W, Jianbo W, Yanhua X. Determination of tryptamine concentration and pharmacokinetic parameters in rat plasma by HPLC. Chin Pharmacol Bull. 2012;28(02):270–4.

32. Heng F, Meng X, Qing T. Research progress in regulation of Th17/Treg cell differentiation in ulcerative colitis by aromatic hydrocarbon receptors and their ligands. World J Chin Digestion. 2015;23(19):3101–8.

33. Kimura A, Naka T, Nohara K, Fujii-Kuriyama Y, Kishimoto T. Aryl hydrocarbon receptor regulates Stat1 activation and participates in the development of Th17 cells. Proc Natl Acad Sci U S A. 2008;105(28):9721–6.

34. Lee CL, Wang CM, Hu HC, Yen HR, Song YC, Yu SJ, Chen CJ, Li WC, Wu YC. Indole alkaloids indigodoles A-C from aerial parts of Strobilanthes cusia in the traditional Chinese medicine Qing Dai have anti-IL-17 properties. Phytochemistry. 2019;162:39–46.

Publisher's note